



**Binuclear heterometallic M(iii)–Mn(ii) (M = Fe, Cr)
oxalate-bridged complexes associated with a
bisamidinium dication: a structural and magnetic study**

Catalin Maxim, Sylvie Ferlay, Cyrille Train

► **To cite this version:**

Catalin Maxim, Sylvie Ferlay, Cyrille Train. Binuclear heterometallic M(iii)–Mn(ii) (M = Fe, Cr) oxalate-bridged complexes associated with a bisamidinium dication: a structural and magnetic study. New Journal of Chemistry, 2011, 35 (6), pp.1254. 10.1039/C0NJ00976H . hal-02301251

HAL Id: hal-02301251

<https://hal.science/hal-02301251>

Submitted on 27 Nov 2020

HAL is a multi-disciplinary open access archive for the deposit and dissemination of scientific research documents, whether they are published or not. The documents may come from teaching and research institutions in France or abroad, or from public or private research centers.

L'archive ouverte pluridisciplinaire **HAL**, est destinée au dépôt et à la diffusion de documents scientifiques de niveau recherche, publiés ou non, émanant des établissements d'enseignement et de recherche français ou étrangers, des laboratoires publics ou privés.

Binuclear heterometallic M(III)–Mn(II) (M = Fe, Cr) oxalate-bridged complexes associated with a bisamidinium dication: a structural and magnetic study

Catalin Maxim,^{a,b} Sylvie Ferlay^{a,c,*} and Cyrille Train^{d,e,*}

5 Received (in XXX, XXX) Xth XXXXXXXXXX 200X, Accepted Xth XXXXXXXXXX 200X

First published on the web Xth XXXXXXXXXX 200X

DOI: 10.1039/b000000x

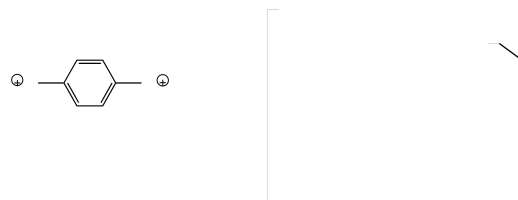
Two heterometallic oxalate-bridged dinuclear anions associated with a non H-bond donor bisamidinium cation, leading to compounds of formula (Cat)[Mn^{II}(H₂O)₄M^{III}(ox)₃]₂·6H₂O (M = Fe (1) and Cr (2)), are presented. Their structural analysis reveals that the anion is the combination of a tris(oxalato)metallate(III) moiety with a tetra(aqua)manganese(II) entity. A 3D H-bonded network is formed between the crystallisation and coordination water molecules and the terminal and bridging oxalate ligands. The exchange interaction between both metal ions mediated by the oxalate bridge is worth -4.9 cm⁻¹ for **1** and +1.6 cm⁻¹ for **2** ($\mathcal{H} = -J S_1 \cdot S_2$).

Introduction

With the recent exciting development of coordination polymers,¹ the understanding of their formation has concentrated recently many interests. In order to elucidate and rationalise this, several model coordination complexes have been synthesised. To illustrate this approach, the family of oxalate-bridged bimetallic compounds,² related to the field of molecular magnetism,³ has provided several series of original compounds of various dimensionalities incorporating a large variety of cations. In the field of extended networks (2D or 3D), several examples of magnetic and/or multifunctional bimetallic oxalate-bridged compounds have been discovered : (i) (6,3) bidimensional bimetallic anionic layers hosting a large variety of cationic guests: spin transition complexes⁴, paramagnetic dexamethylferrocenium⁵, photochromic molecules,⁶ nonlinear optical (NLO)-active molecules,⁷ organic π -electron donors,⁸ chiral cations,⁹ etc... and (ii) (10,3) three-dimensionnal bimetallic anionic network¹⁰, not as versatile as 2D networks, which can also welcome cationic functional guests, that lead to remarkable physico-chemical properties.¹¹

Isolated oxalate-bridged polynuclear complexes have also been intensively studied.¹² For example, trinuclear anionic complexes have been formed when associated with TTF,¹³ redox-active bipyridinium¹⁴ or polar¹⁵ cations. The case of dinuclear coordination complexes have been encountered more scarcely. Two dimeric complexes involving the [M^{III}(ox)₃]³⁻ anion are reported : they are related to compounds displaying a monodentate coordination mode of the oxalate between metal centers.¹⁶ A dimeric homometallic compound, where the bis-bidentate coordination mode of oxalate occurs, has also been reported.¹⁷ Beside this, there are few bimetallic complexes presenting blocking ligands^{18,19} that are used to prevent willingly the formation of extended networks.

In all cases, the formation of bimetallic species is related to the use of counter cations. Cyclic cationic amidinium are good candidates for this approach. They have recently been used for building extended hydrogen bonded (H-bonded) networks²⁰ with poly(thiocyanoato)metallate,²¹ poly(oxalato)metallate²² or poly(cyanido)metallate.²³ Some of the reported crystalline H-bonded networks exhibit luminescence²⁴, porosity²⁵ or liquid crystalline behaviour.²⁶ When these cations are not involved in H-bonds with anionic units, the formed compounds can behave as ionic liquids, as recently shown.²⁷ Here we report our first efforts to build up oxalate-bridged architectures in association with a dication (Cat²⁺) based on cyclic bisamidinium. Two heterometallic compounds of formula Cat[Mn^{II}(H₂O)₄M^{III}(ox)₃]₂·6H₂O (M = Fe (**1**) and Cr (**2**)) have been obtained (Scheme 1). They are based on the [M^{III}(ox)₃]³⁻ (M = Fe and Cr) building block, where oxalate presents a bisbidentate coordination mode towards Mn(II). Compound **1** is the first Mn-Fe oxalate-bridged oligonuclear complexes to be reported. This is of importance in the understanding of the exchange interaction in Mn-Fe oxalate-bridged compounds. The complexes have been characterized from a structural point of view and their magnetic properties have been analysed.



Scheme 1 : Schematic representation of the used cation (left) and of the obtained anionic bimetallic dinuclear unit with M = Fe or Cr (right).

Results and discussion

1) Structural analysis

Compounds **1** and **2** were obtained as crystalline materials and revealed to be isomorphous (monoclinic, $P2_1/n$). The asymmetric unit has one half of an amidinium dication lying about an inversion center with one anionic dimeric units $[(H_2O)_4Mn^{II}(ox)M^{III}(ox)_2]^-$ and three water molecules in general positions (Fig. 1). A summary of the crystallographic data for **1** and **2** are listed in Table 1 and selected bond distances and angles for **1** and **2** are presented in ESI. In the following, since both compounds **1** and **2** are isomorphous, we will focus on the description of the structure of **1**.

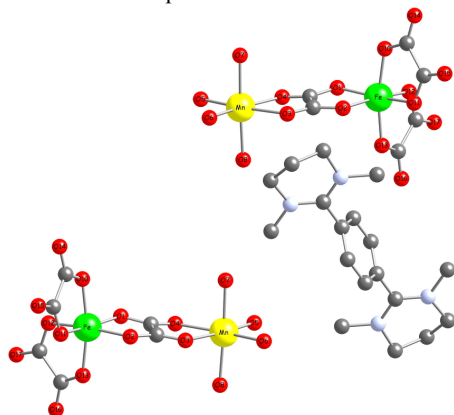


Figure 1 : Dicationic and anionic units in compound **1** together with the numbering scheme.

Table 1 : Crystallographic Parameters for **1** and **2** recorded at 173K.

Formula	1	2
	$C_{15}H_{28}FeMnN_2O_{19}$	$C_{15}H_{28}CrMnN_2O_{19}$
Molecular weight	651.18	647.33
Crystal system	Monoclinic	Monoclinic
Space group	$P2_1/n$	$P2_1/n$
a(Å)	9.0124(2)	9.0030(2)
b(Å)	19.4857(4)	19.3913(5)
c(Å)	14.4710(3)	14.5081(4)
β (deg)	96.089(1)	96.087(1)
V(Å ³)	2526.96(9)	2518.54(11)
Z	4	4
Colour	green	violet
Crystal dim (mm ³)	0.15x0.05x0.05	0.1x0.06x0.03
D _{calc} (gcm ⁻³)	1.712	1.707
F(000)	1340	1332
μ (mm ⁻¹)	1.165	1.024
Wavelength (Å)	0.71073	0.71073
Number of data meas.	21357	15487
Number of data with I>2 σ (I)	7379 [R(int) = 0.0222]	4875 [R(int) = 0.0416]
R	R1 = 0.0275, wR2 = 0.0736	R1 = 0.0862, wR2 = 0.2217
R _w	R1 = 0.0370, wR2 = 0.0799	R1 = 0.0920, wR2 = 0.2316
GOF	0.868	1.015
Largest peak in final difference (eÅ ⁻³)	-0.335 and 0.504	-0.826 and 1.262

For the anionic $[(H_2O)_4Mn^{II}(ox)M^{III}(ox)_2]^-$ moiety, both metal centres present a slightly distorted octahedral geometry. The manganese(II) ion presents an O6 environment resulting from four coordinated water molecules and two oxygen atoms from the oxalate bridge. The Mn-O distances vary between 2.1418(11)Å and 2.1656(12)Å for water molecules and 2.2424(11)Å and 2.1325(12)Å for the oxalate bridge. This is typical of the +II oxidation state of manganese. The O-Mn-O

angles vary between 75.41(5) and 96.84(6)°. The iron(III) ion is surrounded by 3 oxalate ligands. The Fe-O distances vary from 1.9838(11)Å and 2.0179(11)Å. These figures are typical of the +III oxidation state of iron. The O-Fe-O angles vary between 80.13(4)° and 96.35(5)°. The C-O distances in the bridging oxalate ligand are equal to 1.2319(17) Å when coordinated to Mn(II), and to 1.2704(17) and 1.2739(17) Å when coordinated to Fe(III). The C-O distance for the terminal oxalate ligands are shorter, varying between 1.2146(19)Å and 1.2238(19)Å, which is typical for what is observed in the $K_3[Fe(ox)_3] \cdot 3H_2O$ salt.²⁸ In the two anionic complexes present in the unit cell, the tris(bischelated)metal centres adopt opposite (*A*) and (*A*) configurations (Fig. 1) in agreement with the observed achiral space group $P2_1/n$. The shortest intra- and inter-molecular M(III)-Mn(II) distances are respectively 5.524 Å and 6.168 Å for the chromium(III) derivatives and 5.478 Å and 6.166 Å for the iron(III) analog.

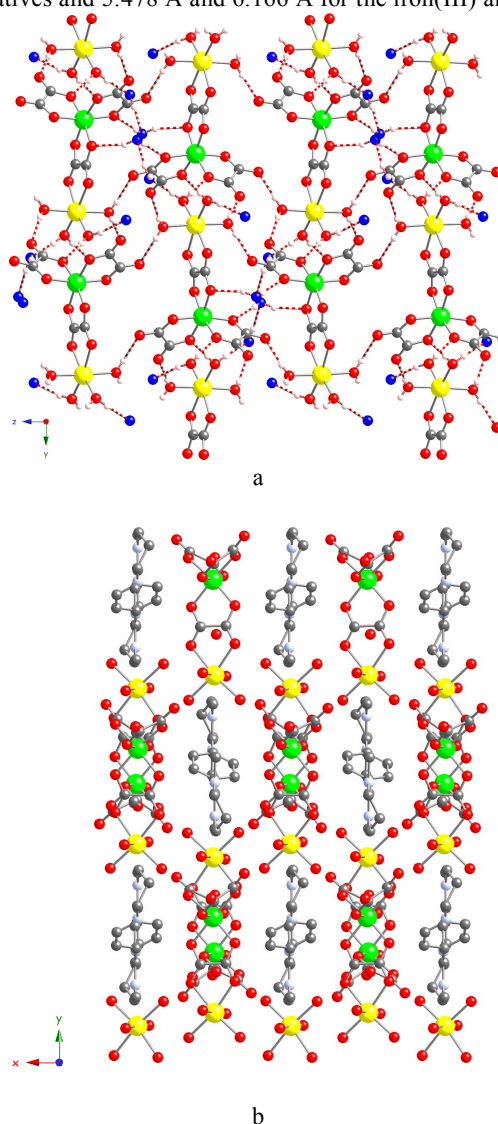


Figure 2 : For compound **1** a) Role of the water molecules in the formed 3D H-bonded network (red around the Mn atoms and blue for the crystallisation water molecules), view in the (100) plane and b) location of the cationic units, view in the (001) plane

Concerning the cationic moieties, the C-N distances vary

between 1.316(2) Å and 1.322(2) Å with the N–C–N angle of 122.38(14)°. These values are close to those observed for analogous H-bond donors bisamidinium compounds.²³ Both six-member amidinium cycles adopt the usual half chair conformation (Fig. 1) and are almost parallel and tilted with respect to the phenyl ring with the NCCC dihedral angle of 104.9°, which confers to them a twisted conformation inside the cavity.

In the network, the anionic species are interconnected into a 3D networks through H-bonds, as shown in figure 2a. All non bonding oxygen atoms of the two terminal oxalate ligands, as well as all oxygen atoms of water molecules surrounding the manganese(II) ion, form H-bonds with O14–O7, O15–O8, O16–O8 and O17–O7 distances of 2.745(2)Å, 2.800(2)Å, 2.743(2)Å and 2.738(2)Å respectively. The resulting 3D H-bonded network presents cavities, where some water molecules are located (Fig. 2a). These water molecules are H-bonded to oxygen atoms of bridging oxalate ligands or to coordinated water molecules with O···O distances varying from 2.684(3)Å and 2.931(19)Å. In these cavities are also located the cationic units (Fig. 2b).

The 3D H-bonded network can be schematized by two non superimposable honeycomb like 2D systems (in the (001) plane) formed by the metals (Mn and Fe), as shown in figure 3.

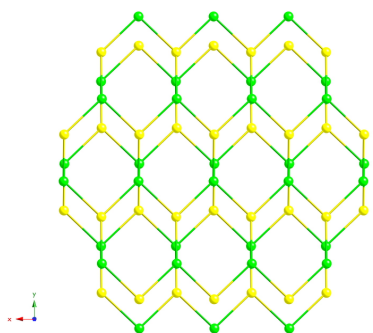


Figure 3 : Projection in the (001) plane of two non superimposable 2D arrays formed by the Fe (green) and Mn (yellow) metals in **1**.

Though a given cation can either lead to a 2D bimetallic oxalate bridged extended network⁸ or to discrete entities,¹³ it is likely that the counter-ion has some influence on the dimensionality through its size, charge and shape. In the present case, we use a large dication whose characteristics, at first sight, can be considered as comparable to those of NLO-active stilbazolium⁷ or organic π -electron donors⁸ that lead to the formation of 2D (6,3) networks. Nevertheless, in the present case, the fact that the used cation may not be engaged in any H-bond with oxalate or solvent molecules, and also a certain flexibility concerning its conformation, influences the formation of the $[(\text{H}_2\text{O})_4\text{Mn}^{\text{II}}(\text{ox})\text{M}^{\text{III}}(\text{ox})_2]^-$ dimeric units. A common feature to all the structures containing discrete oxalate-bridged complexes is the presence of numerous H-bonds between the water molecules coordinated to manganese(II) with the terminal oxalate groups of the tris(oxalato)metalate(III) moiety of neighbouring complexes as well as with crystallisation water molecules present in the network (figure 2), leading the formation of a 3D H-bonded network.

50 2) Magnetic properties

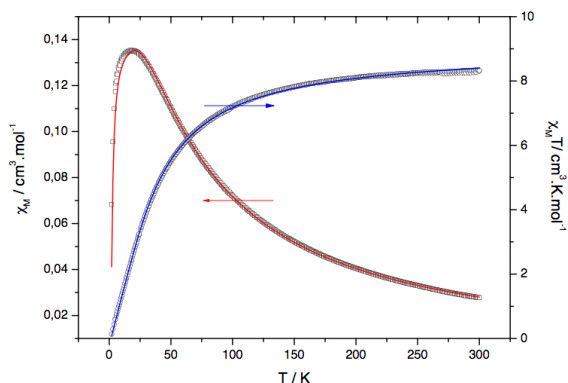


Figure 4 : Thermal variations of the magnetic susceptibility χ_M (□; left axis) and $\chi_M T$ (○; right axis) product for **1**, the solid lines being the best-fit curves (see text).

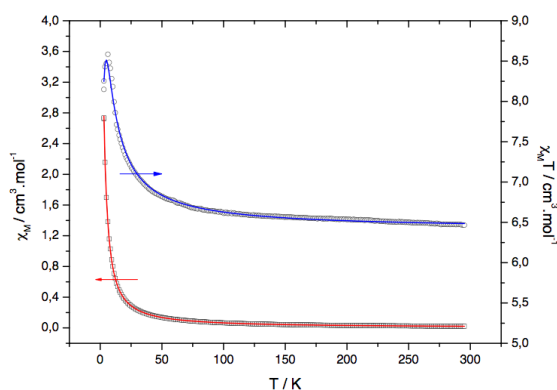


Figure 5 : Thermal variations of the magnetic susceptibility χ_M (□; left axis) and $\chi_M T$ (○; right axis) product for **2**, the solid lines being the best-fit curves (see text).

55

The thermal variations of the molar magnetic susceptibility per dinuclear unit, χ_M , and of the $\chi_M T$ product for **1** and **2** are shown in figures 4 and 5 respectively. At room temperature (RT), the $\chi_M T$ values are worth 8.34 and 6.46 $\text{cm}^3 \text{mol}^{-1} \text{K}$ for **1** and **2**, respectively. For **1**, it is slightly lower than the spin-only values ($g=2$) expected for the two high spin $S=5/2$ ($\chi_M \cdot T = 8.75 \text{ cm}^3 \cdot \text{K} \cdot \text{mol}^{-1}$) while, for **2**, it is slightly higher than the value expected for one $S=3/2$ center and one high spin $S=5/2$ center ($\chi_M T = 6.25 \text{ cm}^3 \cdot \text{K} \cdot \text{mol}^{-1}$). When the temperature decreases, the magnetic susceptibility of **1** increases until it reaches a maximum of *ca* 0.135 $\text{cm}^3 \cdot \text{mol}^{-1}$ at 21 K and then decreases abruptly. Accordingly, its $\chi_M T$ product displays a monotonous decrease with an increasing rate from RT down to 2 K. The magnetic behaviour observed for **2** is rather different: its magnetic susceptibility increases monotonously with a continuously increasing rate from RT down to 2 K while its $\chi_M T$ product exhibits a sharp maximum of 8.58 $\text{cm}^3 \cdot \text{K} \cdot \text{mol}^{-1}$ at 6.2 K before decreasing abruptly. The overall magnetic behaviour of $[(\text{H}_2\text{O})_4\text{Mn}^{\text{II}}(\text{ox})\text{Fe}^{\text{III}}(\text{ox})_2]^-$ (**1**) and

75

$[(\text{H}_2\text{O})_4\text{Mn}^{\text{II}}(\text{ox})\text{Cr}^{\text{III}}(\text{ox})_2]^-$ (**2**) is indicative of an antiferromagnetic (AF) and a ferromagnetic (F) exchange interaction between the spin bearers, respectively. Such interactions lead to a $S=0$ and $S=3/2+5/2=4$ ground spin state for **1** and **2** respectively. Accordingly, the $\chi_{\text{M}}T$ product at low temperature falls to 0 for **1** while the maximum value of $8.58 \text{ cm}^3\cdot\text{K}\cdot\text{mol}^{-1}$ observed for **2** is lower than the value expected of $10.0 \text{ cm}^3\cdot\text{K}\cdot\text{mol}^{-1}$ for a $S=4$ with $g=2$. The abrupt decrease below 6.2 K is indeed the signature of either AF intermolecular interactions or zero field splitting of the $S=4$ ground state. Both phenomena have comparable phenomenological influence on the macroscopic magnetic behaviour of powder samples: they prevent reaching the value expected for an isotropic $S=4$ ground state. The former phenomenon is arbitrarily favoured through the analysis of the magnetic data.

To provide a quantitative analysis, we describe the system by using an isotropic spin Hamiltonian given by eq. (1.1) for dinuclear complexes. The first term accounts for the intramolecular exchange interaction while the second one treats the intermolecular interactions in the mean field approximation. Eq. (1.1) is used to obtain analytical expressions of the magnetic susceptibility where the second term appears as a correction to the temperature through a Curie-Weiss temperature which is related to the zj by eq. (1.2).^{3,18}

$$\mathcal{H} = -J \mathbf{S}_{\text{Mn}} \cdot \mathbf{S}_{\text{M}} - zj \langle S_z \rangle S_z \quad (1.1)$$

$$\theta = zjS(S+1)/3k \quad (1.2)$$

Table 2 :Best-fit magnetic parameters for **1** and **2**

Complex	J^a / cm^{-1}	θ^b / K	g^c	Θ
1 (Mn-Fe)	-4.9	0	2.02	-62 ^d
2 (Mn-Cr)	+1.6	-0.67	2.21	+13 ^d
[Mn-Fe] network				-86,-146 ³¹
[Mn-Cr] network	+0.5			+6,+9.3 ^{2,9a,32}

^a Intramolecular magnetic exchange coupling. ^bCurie-Weiss temperature (see eq. (2.1)). ^cAveraged Landé factor. ^dCalculated from J using the generalised version of eq. (1.2).¹⁸

To improve the robustness of the fit, it has been performed simultaneously on the thermal variations of χ_{M} and $\chi_{\text{M}}T$ product, as shown in Fig. 4 and 5.²⁹ The parameters deduced from the fit of the experimental data of **1** and **2** are summarised in table 2. As anticipated from the qualitative analysis, the intramolecular exchange interaction is AF for **1** and F for **2**. Following the $S=0$ ground state for **1**, the Curie-Weiss temperature is zero (eq. (1.2)). On the contrary, the negative Curie-Weiss temperature (-0.67 K) observed for **2** is indicative of AF intermolecular interactions between the $S=4$ ferromagnetically coupled dinuclear complexes and/or ZFS of the $S=4$ ground state of these species. The weak intermolecular exchange interactions are mediated by the H-bonds network between the dinuclear complexes. The nature of the exchange observed in **2** corresponds to previously reported experimental results on oxalate-bridged oligonuclear complexes.^{15,18} Its intensity is slightly higher than the previously reported values. Since J results from the competition between the F $(\text{t}_{2\text{g}})^3(\text{Cr})-(\text{e}_{\text{g}})^2(\text{Mn})$ and AF

$(\text{t}_{2\text{g}})^3(\text{Cr})-(\text{t}_{2\text{g}})^3(\text{Mn})$ exchange pathways across the oxalate bridge,³⁰ slight modifications of the structure and, hence, of the electronic structure can justify this small increase. Due to the low value of the overall exchange interaction and the existence of competing interactions, we are in borderline cases where sophisticated calculations do not necessarily reproduce the experimental observations¹⁵ preventing a complete rationalisation of the intramolecular interaction. The AF exchange interaction observed in complex **1** cannot be directly compared to other discrete complexes since there is no previous report on oxalate-bridged oligonuclear $[\text{Mn}(\text{II})-\text{Fe}(\text{III})]$ complexes. Nevertheless, it is interesting to compare them with $[\text{Fe}(\text{III})-\text{Fe}(\text{III})]$ oxalate-bridged homometallic dinuclear complexes^{17b,e} because both have a d^5-d^5 electronic structure. We indeed find here a decrease of the exchange interaction that reaches 25% compared to the homometallic analogues though the intramolecular metal-metal distance is much comparable. Following the magnetic orbitals analysis introduced by late O. Kahn,³ this decrease can be attributed to the mismatch between the energy levels introduced by the heterometallic nature of the complex thus reducing the efficiency of the AF exchange pathways.

A second attractive approach proposed by Ohba *et al.* consists in comparing the J values obtained for discrete oligonuclear complexes with the Curie-Weiss temperatures found for oxalate-bridged $[\text{Mn}-\text{M}]$ triconnected extended networks by using the generalised version of eq. (1.2).¹⁸ Following this procedure, we calculate a value of -62 K and +13 K for a (6,3) network derived from the J values obtained for **1** and **2** respectively. The former value is below those observed by Mathonière *et al.*³¹ for a eight-members series of 2D oxalate-bridged $[\text{Mn}-\text{Fe}]$ networks (Table 2) while the latter is higher than the value observed in $[\text{Mn}-\text{Cr}]$ networks.^{2,9a,32} This discrepancy contrasts with the excellent agreement between the J values of a series of $[\text{M}-\text{Cr}]$ ($\text{M}=\text{Mn}, \text{Fe}, \text{Co}, \text{Ni}, \text{Cu}$) dinuclear complexes and the Curie temperatures T_{C} of the corresponding 2D networks found by Ohba *et al.*¹⁸ But, in their study: (i) the authors compare the J values deduced from a fit using spin Hamiltonians written $-2J \mathbf{S}_1 \cdot \mathbf{S}_2$ with a J_{cal} deduced from T_{C} assuming that the exchange interaction is defined as $-J \mathbf{S}_1 \cdot \mathbf{S}_2$; J_{cal} is thus overestimated by a factor of 2 (ii) in the mean-field approach the absolute value of the Curie-Weiss (Θ) and the ordering temperatures (T_{C}) are equal while a more sophisticated approach leads to $T_{\text{C}} < |\Theta|$. This is particularly true for AF coupled networks. It thus appears that the approach proposed by Ohba *et al.*¹⁸ can only be considered as a rough mean to compare the magnetic properties observed in extended networks and discrete complexes. Nevertheless, it allows (i) to underline the respective role of the exchange parameter J and of the value of the spin of the paramagnetic centres in the T_{C} value (ii) to anticipate from the study of discrete compounds the main trends that can be expected for the related extended networks.

Conclusions

Using a non H-bond donor bisamidinium dication, two isomorphous oxalate-bridged dinuclear complexes containing a tris(oxalato)metalate(III) moiety in a bis-bidentate

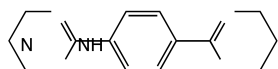
coordination mode were obtained. Moreover, the structure reveals a 3D H-bonded network related to the role played by the water molecules. The magnetic properties indicate a AF intramolecular exchange interaction between manganese(II) and iron(III) centers while it is F when the iron(III) is replaced by chromium(III). The absolute intensity of the former is 5 times the one of the latter. In both cases, these properties reflects those observed for analogous extended networks,^{31,32} the role played by the environment (water molecules) being negligible.

Though it is not the only parameter to control the dimensionality of the formed oxalate bridged bimetallic compound, we intend to adjust the nature (shape, size, charge) of the used amidinium cation to favour the formation of tunable extended networks exhibiting long-range magnetic ordering. This will allow the magnetic properties of the networks with the physico-chemical properties arising from the cation.²¹⁻²³

Experimental part

Synthesis

The $\text{MnCl}_2 \cdot 4\text{H}_2\text{O}$ and $\text{K}_3[\text{Fe}(\text{ox})_3] \cdot 3\text{H}_2\text{O}$ were purchased from commercial sources and used as received. $\text{K}_3[\text{Cr}(\text{ox})_3] \cdot 3\text{H}_2\text{O}$ ³³ and starting compound **A** (Scheme 2) were prepared following the literature procedures.^{23a, 25}



Scheme 2 : Representation of the starting compound **A**.

Synthesis of $\text{cat}^{2+}\text{-2I}^-$:³⁴

A mixture of compound **A** (1.19 g, 4.92 mmol), NaH (271 mg, 11.3 mmol) in DMF (100 mL) was stirred at RT. After 2 hours, MeI (2.93 g, 20.66 mmol) was added to the solution and heated to 75 °C during 15 hours. The resulting solution was washed with 100 mL water and with 10 mL Et_2O .

$\text{cat}^{2+}\text{-2I}^-$ was obtained in 70% yield upon recrystallisation from distilled water. Mp: 182 °C (decomposition at 230°C).

¹H-NMR (D_2O , δ ppm): 2.141 (q, 4H, $\text{CH}_2(\text{CH}_2\text{-N})_2$), 2.779 (s, 12H, $\text{CH}_3\text{-N}$), 3.502 (m, 8H, $\text{CH}_2\text{-N}$), 7.631 (s, 4H, CH arom.); ¹³C-NMR (CD_3OD , δ ppm): 22.1 (N- $\text{CH}_2\text{-CH}_2\text{-CH}_3\text{-N}$), 39.2 ($\text{CH}_3\text{-N}$), 47.7 ($\text{CH}_2\text{-N-CH}_3$), 126.8 (CH arom.), 135.4 (CH arom.), 159.0 (N-C-N). Elemental analysis : $\text{C}_{18}\text{H}_{30}\text{N}_4\text{I}_2$: calculated : C = 48.13%, H = 6.06%, N = 14.03% ; found: C = 47.6%, H = 5.66%, N = 13.78%.

Synthesis of **1** and **2**:

Compounds **1** and **2** were obtained as green (**1**) and violet (**2**) crystals by slow evaporation at room temperature (2 weeks) of an aqueous solution (10 mL) containing $\text{K}_3[\text{M}(\text{ox})_3] \cdot 3\text{H}_2\text{O}$ (123 mg for M =Fe and 122 mg for M =Cr, 0.25 mmol), $\text{MnCl}_2 \cdot 4\text{H}_2\text{O}$ (50 mg, 0.25 mmol) and $\text{cat}^{2+}\text{-2I}^-$ (69 mg, 0.125 mmol). Yield : ca. 80% for **1** and **2**.

Elemental analysis for $\text{C}_{15}\text{H}_{28}\text{FeMnN}_2\text{O}_{19}$ (**1**): calculated: C = 27.67%, H = 4.33%, N = 4.30%; found: C = 27.55%, H = 4.24%, N = 4.19%; IR: 3423 (O-H), 3243, 3045 and 2956 (C-H), 1701, 1663, 1638 (C=O) cm^{-1} .

Elemental analysis for $\text{C}_{15}\text{H}_{28}\text{CrMnN}_2\text{O}_{19}$ (**2**): calculated: C =

27.83%, H = 4.36%, N = 4.33%, H 4.19%, N 4.21%; IR: 3336 (O-H), 3045 and 2925 (C-H), 1701, 1666, 1639 (C=O) cm^{-1} .

The purity of the obtained polycrystalline samples has been evidenced by PXRD measurements (see fig. S1, ESI). The TGA measurements are also presented in ESI. (see fig. S2, ESI)

Single-Crystal Studies.

Data were collected at 173(2) K on a Bruker APEX8 CCD Diffractometer equipped with an Oxford Cryosystem liquid N_2 device, using graphite-monochromated Mo-K α ($\lambda = 0.71073$) radiation. The structures were solved by direct methods and refined by full-matrix least squares techniques based on F^2 . The non-H atoms were refined with anisotropic displacement parameters. Calculations were performed using SHELX-97 crystallographic software package. All hydrogen atoms were generated geometrically with the exception of the hydrogen atoms of the water molecules. The hydrogen atoms of the water molecules were located on a ΔF map and refined with restraints.³⁵

CCDC 804356 and CCDC 804357 contain supplementary crystallographic data for **1** and **2** respectively. They can be obtained free of charge from the Cambridge Crystallographic Data Centre via www.ccdc.cam.ac.uk/datarequest/cif.

Physical techniques

Diagrams were collected on a Bruker D8 diffractometer using monochromatic Cu-K α radiation with a scanning range between 3.8 and 30° using a scan step size of 2°/mn. TGA measurements have been performed on polycrystalline compounds on Pyris 6 TGA Lab System (Perkin-Elmer), using a N_2 flow of 20 mL/mn and a heat rate of 4°C/mn. Variable temperature (2.0-300 K) magnetic susceptibility measurements were carried out on polycrystalline samples with a MPMS SQUID magnetometer by applying a 1500 G external magnetic field.

Acknowledgement

Pr. M. W. Hosseini is warmly acknowledged for fruitful discussions. This work was supported by the Centre National de la Recherche Scientifique (CNRS), Université de Strasbourg (UdS), Université Joseph Fourier (UJF) and the Agence Nationale de la Recherche (ANR) within the framework of the ANR-08-JCJC-0113-01 project in particular through a postdoctoral grant to C. M.

Notes and references

^a Laboratoire de Chimie de Coordination Organique, UMR CNRS-UdS 7140, Université de Strasbourg, Institut Le Bel, 4, rue Blaise Pascal, F-67000 Strasbourg, France

^b University of Bucharest, Faculty of Chemistry, Inorganic Chemistry Laboratory, Str. Dumbrova Rosie nr. 23, 020464-Bucharest, Romania.

^c Institut Universitaire de France (IUF)

^d Laboratoire National des Champs Magnétiques Intenses, UPR CNRS 3228, 25 rue des Martyrs, B.P. 166, 38042 Grenoble cedex 9, France

^e Université Joseph Fourier, BP 53, F-38041 Grenoble Cedex 9, France
E-mail : cyrille.train@grenoble.cnrs.fr, ferlay@unistra.fr

† Electronic Supplementary Information (ESI) available: PXRD characterization of **1** and **2**, as well as TGA data. Selected bond distances and angles for **1** and **2**.

5 See DOI: 10.1039/b000000x/

- 1 (a) S. R. Batten and R. Robson, *Angew. Chem., Int. Ed.*, 1998, **37**, 1460; (b) A. J. Blake, N. R. Champness, P. Hubberstey, W.-S. Li, M. A. Withersby and M. Schröder, *Coord. Chem. Rev.*, 1999, **183**, 117; (c) G. F. Swiegers and T. J. Malefetse, *Chem. Rev.*, 2000, **100**, 3483; (d) M. Eddaoudi, D. B. Moler, H. Li, B. Chen, T. M. Reineke, M. O'Keefe and O. M. Yaghi, *Acc. Chem. Res.*, 2001, **34**, 319; (e) C. Janiak, *Dalton Trans.*, 2003, 2781; (f) S. Kitagawa, R. Kitaura and S. I. Noro, *Angew. Chem., Int. Ed.*, 2004, **43**, 2334; (g) G. Férey, C. Mellot-Draznieks, C. Serre and F. Millange, *Acc. Chem. Res.*, 2005, **38**, 217; (h) D. MasPOCH, D. Ruiz-Molina and J. Veciana, *Chem. Soc. Rev.*, 2007, **36**, 770.
- 2 R. Clément, S. Decurtins, M. Gruselle and C. Train, *Monatsh. Chem.* 2003, **134**, 117.
- 3 O. Kahn, *Molecular Magnetism*, VCH, New York, 1993.
- 4 (a) M. Clemente-León, E. Coronado, M. C. Giménez-López, A. Soriano-Portillo, J. C. Waerenborgh, F. Delgado and C. Ruiz-Pérez *Inorg. Chem.* 2008, **47**, 9111; (b) M. Clemente-León, E. Coronado, M. López-Jordà, G. Minguez Espallargas, A. Soriano-Portillo and J. C. Waerenborgh *Chem. Eur. J.* 2010, **16**, 2207
- 5 (a) M. Clemente-León, J. R. Galán-Mascarós and C. J. Gómez-García, *Chem. Commun.* 1997, 1727; (b) E. Coronado, J. R. Galán-Mascarós, C. J. Gómez-García and J. M. Martínez-Agudo, *Adv. Mater.* 1999, **11**, 558
- 6 (a) S. Bénard, P. Yu, J. P. Audière, E. Rivièrè, R. Clément, J. Ghillem, L. Tchertanov and K. Nakatani, *J. Am. Chem. Soc.* 2000, **122**, 9444; (b) S. M. Aldoshin, N. A. Sanina, V. I. Minkin, N. A. Voloshin, V. N. Ikorskii, V. I. Ovcharenko, V. A. Smirnov and N. K. Nagaeva, *J. Mol. Struct.* 2007, **826**, 69.
- 7 M. Gruselle, B. Malézieux, S. Bénard, C. Train, C. Guyard-Duhayon, P. Gredin, K. Tonsuaadu and R. Clément, *Tetrahedron Asym.* 2004, **15**, 3103.
- 8 (a) M. Kurmoo, A. W. Graham, P. Day, S. J. Coles, M. B. Hursthouse, J. L. Caulfield, J. Singleton, F. L. Pratt and W. Hayes, *J. Am. Chem. Soc.* 1995, **117**, 12209; (b) E. Coronado, J. R. Galán-Mascarós, C. J. Gómez-García and V. Laukhin, *Nature* 2000, **408**, 447
- 9 (a) C. Train, R. Gheorghe, V. Krstic, L. M. Chamoreau, N. S. Ovanesyan, G. L. J. A. Rikken, M. Gruselle and M. Verdager, *Nat. Mater.* 2008, **7**, 729; (b) C. Train, T. Nuida, R. Gheorghe, M. Gruselle and S.-I. Ohkoshi, *J. Am. Chem. Soc.* 2009, **131**, 16838.
- 10 (a) S. Decurtins, H. W. Schmalle, P. Schneuwly and H. R. Oswald, *Inorg. Chem.* 1993, **32**, 1888; (b) S. Decurtins, H. W. Schmalle, P. Schneuwly, J. Ensling and P. Gülich, *J. Am. Chem. Soc.* 1994, **116**, 9521; (c) M. Hernández-Molina, F. Lloret, C. Ruiz-Pérez and M. Julve, *Inorg. Chem.* 1998, **37**, 4141; (d) E. Coronado, J. R. Galán-Mascarós, C. J. Gómez-García and J. M. Martínez-Agudo, *Inorg. Chem.* 2001, **40**, 113; (e) M. Gruselle, R. Andrés, B. Malézieux, M. Brissard, C. Train and M. Verdager, *Chirality*, 2001, **13**, 712; (f) F. Pointillart, C. Train, F. Villain, C. Cartier dit Moulin, P. Gredin, L.-M. Chamoreau, M. Gruselle, G. Aullon, S. Alvarez and M. Verdager, *J. Am. Chem. Soc.*, 2007, **129**, 1327; (g) M. Clemente-León, E. Coronado, C. J. Gómez-García and A. Soriano-Portillo, *Inorg. Chem.*, 2006, **45**, 5653.
- 11 (a) M. E. von Arx, E. Burattini E, A. Hauser, L. van Pieterson, R. Pellaux and S. Decurtins, *J. Phys. Chem. A* 2000, **104**, 883; (b) R. Sieber, S. Decurtins, H. Stoeckli-Evans, C. Wilson, D. Yufit, J. A. K. Howard, S. C. Capelli and A. Hauser, *Chem. Eur. J.* 2000, **6**, 361.
- 12 G. Marinescu, M. Andruh, F. Lloret and M. Julve, *Coord. Chem. Rev.*, 2011, **255**, 161.
- 13 (a) E. Coronado, J. R. Galán-Mascarós, C. Giménez-Saiz, C. J. Gómez-García, C. Ruiz-Pérez and S. Triki, *Adv. Mater.*, 1996, **8**, 737; (b) E. Coronado, J. R. Galán-Mascarós, C. Giménez-Saiz, C. J. Gómez-García and C. Ruiz-Pérez, *Eur. J. Inorg. Chem.*, 2003, 2290;
- 14 Y.-Q. Sun, J. Zhang, G.-Y. Yang, *Dalton Trans.*, 2006, **35**, 1685.
- 15 E. Pardo, C. Train, R. Lescouëzec, K. Boubekeur, E. Ruiz, F. Lloret and M. Verdager *Dalton Trans.*, 2010, **39**, 4951.
- 16 (a) O. Costisor, K. Mereiter, M. Julve, F. Lloret, Y. Journaux, W. Linert and M. Andruh *Inorg. Chim. Acta*, 2001, **324**, 352 ; (b) S. Nastase, C. Maxim, F. Tuna, C. Duhayon, J.-P. Sutter and M. Andruh *Polyhedron*, 2009, **28**, 1688.
- 17 (a) V. M. Masters, C. A. Sharrad, P.V. Bernhardt, L. R. Gahan, B. Moubaraki and K. S. Murray, *J. Chem. Soc., Dalton Trans.*, 1998, 413; (b) D. Armentano, G. De Munno, J. Faus, F. Lloret and M. Julve *Inorg. Chem.* 2001, **40**, 655; (c) E. Coronado, J. R. Galán-Mascarós and C. J. Gómez-García, *J. Chem. Soc., Dalton Trans.*, 2000, 205; (d) S. Rachid, S. Turner, P. Day, M. E. Light and M. B. Hursthouse, *Inorg. Chem.* 2000, **39**, 2426; (e) D. Armentano, G. De Munno, F. Lloret, M. Julve M, *CrystEngComm*, 2005, **7**, 57.
- 18 M. Ohba, H. Tamaki, N. Matsumoto and H. Okawa, *Inorg. Chem.*, 1993, **32**, 5385.
- 19 (a) R. Lescouëzec, G. Marinescu, J. Vaissermann, F. Lloret, J. Faus, M. Andruh and M. Julve, *Inorg. Chim. Acta*, 2003, **350**, 131 ; (b) G. Marinescu, D. Visinescu, A. Cucos, M. Andruh, Y. Journaux, V. Kravtsov, Y. A. Simonov and Janusz Lipkowski *Eur. J. Inorg. Chem.* 2004, 2914 ; (c) S. Nastase, F. Tuna, C. Maxim, C. A. Muryn, N. Avarvari, R. E. P. Winpenny and M. Andruh *Cryst. Gr. & Des.*, 2007, **7**, 1825.
- 20 S. Ferlay and M. W. Hosseini in "Functional supramolecular architectures for organic electronics and nanotechnology" Eds. P. Samorì and F. Cacialli, Wiley-VCH, 2010
- 21 G. Marinescu, S. Ferlay, N. Kyritsakas and M.W. Hosseini, *Dalton Trans.*, 2008, 615.
- 22 C. Paraschiv, S. Ferlay, N. Kyritsakas, J.-M. Planeix and M. Andruh, *Rev. Roum. Chim.*, 2007, **52**, 101
- 23 (a) S. Ferlay, V. Bulach, O. Félix, M. W. Hosseini, J.-M. Planeix and N. Kyritsakas, *CrystEngComm*, 2002, 447; (b) S. Ferlay, R. Holakovsky, M. W. Hosseini, J.-M. Planeix and N. Kyritsakas, *Chem. Commun.*, 2003, 1224; (c) P. Dechambenoit, S. Ferlay, M. W. Hosseini and N. Kyritsakas, *Chem. Commun.*, 2007, 4626.
- 24 (a) C. Paraschiv, S. Ferlay, V. Bulach and J.-M. Planeix, *Chem. Commun.*, 2004, 2270; (b) P. Dechambenoit, S. Ferlay, N. Kyritsakas and M. W. Hosseini, *CrystEngComm.*, 2011, DOI: 10.1039/c0ce00607f.
- 25 P. Dechambenoit, S. Ferlay, M. W. Hosseini and N. Kyritsakas, *J. Am. Chem. Soc.*, 2008, **130**, 17106.
- 26 P. Dechambenoit, S. Ferlay, B. Donnio, D. Guillon and M. W. Hosseini, *Chem. Commun.*, 2011, 734.
- 27 P. Dechambenoit, S. Ferlay, N. Kyritsakas and M. W. Hosseini, *New J. Chem.*, 2010, **34**, 1184.
- 28 R. Wartchow, *Z. Kristallogr.* 1997, **212**, 83.
- 29 S. Altmannshofer, E. Herdtweck, F. H. Köhler, R. Miller, R. Mölle, E.-W. Scheidt, W. Scherer and C. Train, *Chem. Eur. J.*, 2008, **14**, 8013
- 30 P. Yu, Y. Journaux and O. Kahn, *Inorg. Chem.* 1989, **28**, 100
- 31 C. Mathonière, C. J. Nuttall, S. G. Carling and P. Day, *Inorg. Chem.*, 1996, **35**, 1201.
- 32 H. Tamaki, Z. J. Zhong, N. Matsumoto, S. Kida, M. Koikawa, N. Achiwa, Y. Hashimoto and H. Okawa, *J. Amer. Chem. Soc.* 1992, **114**, 6974
- 33 J. M. Baylar and E. M. Jones in *Inorganic Synthesis*; Ed: H. S. Booth, McGraw-Hill, New York, 1939.
- 34 P. Dechambenoit, Ph.D., Université Louis Pasteur, 2008.
- 35 G. M. Sheldrick, Programs for the Refinement of Crystal Structures, University of Göttingen, Göttingen, Germany, 1996.